[PROC. OF JSCE No. 348/V-1 (Concrete Eng. and Pavements) August 1984]

EXPERIMENTAL AND THEORETICAL STUDIES ON THE BEHAVIORS OF FLEXURALLY RESTRAINED REINFORCED CONCRETE MEMBERS SUBJECTED TO TEMPERATURE GRADIENT

By Ryoichi. SATO, Yukio. AOYAGI** and Tsutom. KANAZU****

The present paper describes the test results of flexurally restrained RC beams subjected to temperature gradients, considering the conditions prevailing in the cylindrical wall and the bottom slab of the RC LNG tanks. Experimentally obtained results concerning flexural rigidities, cracking behaviors, etc. are discussed comparing with those under room temperature.

The theoretical approach previously proposed by the authors is expanded to the cases in which RC members are flexurally restrained under temperature crossfall. The comparison of the theoretical results with those obtained from the experiments confirmed the validity of the proposed method, provided the temperature dependent material properties are to be taken into consideration.

1. INTRODUCTION

Reinforced concrete tanks for storage of liquefied natural gas (LNG) are subjected to extraordinary loading conditions including exposure to extremely low temperature as well as to the temperature difference between inner and outer faces. A number of experimental researches to clarify the effect of extremely low temperature on the mechanical properties of concrete and reinforcing materials as well as reinforced concrete (RC) members have so far been conducted[1)~3)]. Most of the researches related to the reinforced concrete members, however, have been limited to the case in which RC members are tested under constant low temperatures, the test results being compared with those obtained under room temperature. Very few works have been conducted placing emphasis on the thermal stress and cracking behaviors of RC beams subjected to temperature gradients in low temperature regions.

When RC members are subjected to temperature gradients in flexurally restrained conditions, bending moments occur, which constitute one of the main design loads determining the amount of reinforcements in the RC structures such as storage tanks for LNG, containments for nuclear reactors, etc.. Therefore, in order to help rationalize the design of such structures, the properties of thermal stress and cracking characteristics should be made clear and appropriate methods of estimating the mechanical behaviors should be established.

Most of the methods hitherto proposed to estimate restraining moments induced by temperature gradients are only applicable to the cases in which RC structures are subjected to temperature difference in the elevated temperature regions ranging from 0° C up to 100 °C.

They are classified into the following three main categories. That is, ①flexural regidities of cracked sections; ACI Specification for RC chimneys[4)], Gurfinkel[5)], Pajuhesh[6)], Larrabbee et al[7)], etc.

* Member of JSCE, Dr. Eng. Associate Professor, Utsunomiya University (2753, Ishiimachi, Ustunomiya-shi, 321)
** Member of JSCE, Dr. Eng. Head of Material Mechanics Section, CRIEPI (1646, Abiko, Abiko-shi, 271-11)
*** Member of JSCE, M. Eng. Research Engineer of Material Mechanics Section, CRIEPI

②flexural regidities based on the gross section, such as ACI Specification for RC silos[8], etc. and ③ average flexural rigidities taking into consideration the contribution of tensile concrete between cracks ; such as Aoyagi et al[9], Inomata[10], Noakowski[11], etc. . For the case of RC members subjected to temperature gradient in the low temperature regions, because of the marked increments in bond as well as tensile strength of concrete, contribution of concrete between the adjacent cracks to flexural rigidities is pronounced. Although from this point of view, the methods belonging to the category ③ seem most suitable, these approaches do not take into account the influences of temperature change on the mechanical properties of concrete as well as the effects of external moments and axial forces, and are not able to predict the cracking behaviors in a satisfactory manner.

The purpose of the present study is to promote rationalization of design of the RC structures for which the thermal load is one of the controlling design factors. The previously proposed theoretical method[3] was improved to calculate the thermal stresses as well as crack widths in RC beams subjected to not only temperature effects but also external forces. Computed results were discussed on the light of experimental evidences.

2. OUTLINE OF THE EXPERIMENTS

(1) Preparation of RC Test Beams

a) Materials : Ordinary Portland cement was used. Coares aggregates were the crushed stones with maximum size, specific gravity and fineness modulus, 20 mm, 2.70 and 6.68, respectively. The fine aggregate was a river sand having a specific gravity of 2.60 and a fineness modulus of 2.75. As a water reducing agent a product of ligunin was used by the weight of 0.25 % of cement. The design strength of concrete was selected as 400 kg/cm^2 (39.2 MPa). The proportions of concrete were as follows ; Water-cement ratio 41.7 %, slump 8±2 cm, air content 3±1 %, and unit cement content 370 kg/m^3.

Deformed bars with a nominal diameter of 16 mm were arranged in the specimens. Young's modulus, yield point and tensile strength of which were 206×10^4 kg/cm^2 (20.2×10^4 MPa), 3 900 kg/cm^2 (382 MPa) and 5 340 kg/cm^2 (523 MPa), respectively,

b) Preparation of specimens : The main properties of the specimens tested are listed in Table 1. Four beam specimens (L Type) were made for the test of restraining flexural deformation due to temperature gradients, and another four (R Type) for the test of pure bending under uniform and constant room temperature.

Configuration and dimensions of the specimens are depicted in Fig. 1. Over-all length of the beam was 380 cm, the central portion (210 cm) of which was designated as the test area, the cross section being 40 cm (heigth) by 20 cm (width). Both ends of the specimen were enlarged to the section of 40 by 40 cm to facilitate fixing of H beams, which were connected to the beam to apply bending moment.

Two kinds of reinforcement ratios were selected, that is, 0.57 % and 1.13 %, taking into account the prevailing reinforcement ratios in the cylindrical wall (0.3~0.6 %) and the bottom slab (0.8~1.2 %) of a LNG tank, respectively. The arrangement of reinforcing bars is illustrated in Fig. 2. Four out of the total eight specimens were kept under uniform compressive stress of 50 kg/cm^2 (4.9 MPa).

Table 1 Properties of the RC Members Tested.

	P (%)	D (mm)	σ_{pr} (kg/cm^2)	T (°C)	Properties of Conc. under NT σ_{cu} (kg/cm^2)	σ_{bu} (kg/cm^2)	σ_{tu} (kg/cm^2)	E_c (×10^4) (kg/cm^2)
L-1	0.57	16	0	TG	639	53.8	34.1	35.8
R-1	0.57	16	0	NT	538	65.3	36.7	34.2
L-2	1.13	16	0	TG	571	47.4	34.3	36.5
R-2	1.13	16	0	NT	519	62.7	36.5	36.2
L-3	0.48	16	50	TG	503	61.1	35.7	31.5
R-3	0.57	16	50	NT	533	65.1	36.6	37.3
L-4	1.13	16	50	TG	560	60.1	32.8	36.2
R-4	1.13	16	50	NT	464	68.7	34.3	33.0

TG : Thermal Gradient under Low Temperature Region
NT : Normal Temperature
p : Reinforcement Ratio
D : Nominal Bar Diameter
σ_{pr} : Uniform Prestressing Stress in Concrete
σ_{cu} : Compressive Strength of Concrete
σ_{bu} : Modulus of Rupture of Concrete
σ_{tu} : Splitting Tensile Strength of Concrete
Ec : Young's Modulus of Concrete

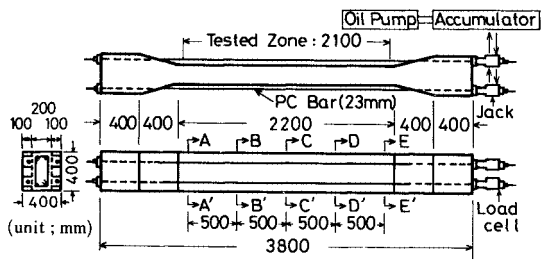

Fig. 1. Configuration and Dimensions of Test Specimens.

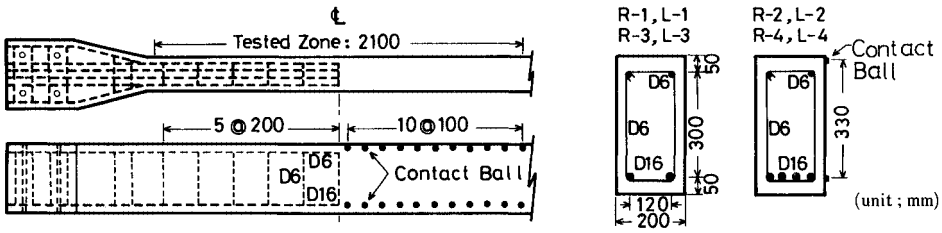

Fig. 2. Arrangement of Reinforcing Bars and Location of Contact Balls.

All the specimens had been cured under water up to 3 or 4 days prior to loading test. For the case of L type specimens, immediately after taking out from under the water the specimens were sealed to prevent evaporation of water with transparent liquid gum which hardens under room temperature. For the case of R type specimens, after the water curing up to the age of 28 days, the specimens were stored in the laboratory room.

(2) Testing Procedures

a) Method of giving temperature gradient to the specimen : As is illustrated in Fig. 3, temperature gradients across the height of the beam were attained in such a manner that the lower face of the specimen was cooled by blowing liquefied nitrogen gas (LN_2), while the temperature of upper face was kept constant by flowing tap water. Both sides of the beam were insulated by foamed stylor plate with a thickness of 10 cm, minimizing the temperature fluctuations across the sides.

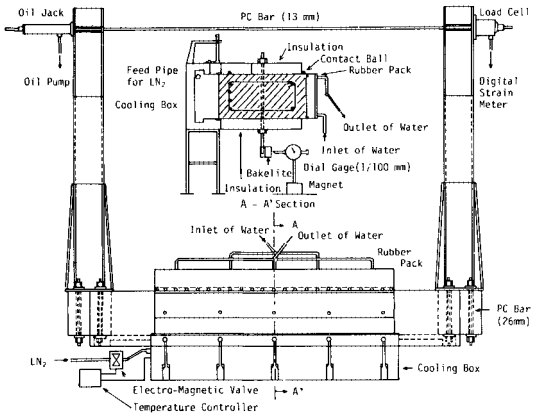

Fig. 3. Apparatus for Restraining Test.

Temperature of the cold face of the specimen was regulated by adjusting the flow of LN_2 using a magnetic valve. The rate of temperature drop was set to be 7～10°C/12 hours and all the measuring operations were conducted after the temperature gradient across the height had been confirmed linear.

b) Methods of applying axial force and restraining moment : Constant axial force was applied by arranging four outer prestressing bars with a diameter of 23 mm, being anchored at the ends of enlarged portion of the beam. Each prestressing bar was tensioned to a constant load of 10 tons.

Restraining moment was determined by the load applied to the prestressing bar which was arranged spanning the open ends of the steel H beams fixed at the ends of the specimen. That is, free warping of the reinforced concrete beam induced by temperature gradients was straightened by tensioning the rod. Thus, the restraining moment, which is originally an internal forces, could be measured as a statical external force. The beam was restrained only flexurally, allowing free axial deformations.

c) Experimental procedures : In the first stage of the experiments free warping test was conducted to determine the average value of thermal expansion coefficients of the specimen. In the second stage the beam was flexurally restrained and measurements were made on restraining moments, crack widths, strains, etc.. In the third stage, flexural restraining test was performed in the condition that constant external moment was superimposed (moment, which stressed the tensile reinforcement to 1 600 kg/cm^2 (157 MPa) calculated by conventional method, except for the L-3 beam, for which the stress caused by external moment was set to be 1 900 kg/cm^2 (186 MPa).). In the final stage, external moment was increased up to failure, keeping the maximum temperature crossfall constant.

During flexural restraining tests, the temperature gradient was increased without giving restraint to the beam in each interval of the measurements. That is, restraining moment was applied only at the time of measurements to minimize the effect of creep.

d) Definition of the restraining moment : Fig. 4 shows the defintion of the restraining moment $M_{\Delta T}$

for the both cases of presence and absence of external moment Mex.

For the case of absence of external moment, the restraining moment is defined as the moment required to straighten the beam with measured free curvature of ϕ_m.

For the case of presence of external moment, taking into account the effect of the residual curvature at the removal of load, the sum of the external and the restraining moment was determined on the measured moment-curvature relationship so as to satisfy the following condition, which represents the increase of curvature corresponding to constant external moment due to the application of the restraining moment;

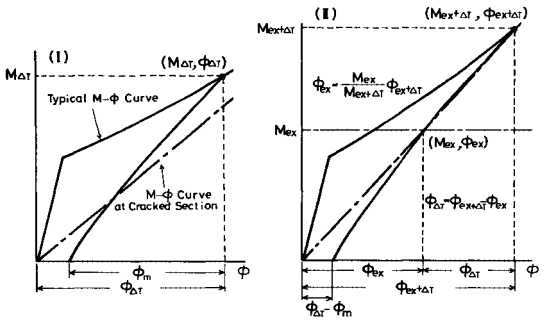

Fig. 4. Definition of Restraining Moment.

$$\phi_{\Delta T}=(1-M_{ex}/M_{ex+\Delta T})\phi_{ex+\Delta T}$$

where :

$\phi_{\Delta T}$: curvature due to temperature crossfall (calculated value assuming $\alpha=10\times10^{-6}/°C$)

α : average thermal expansion coefficient of the test specimens

M_{ex} : externally applied fixed moment

$M_{\Delta T}$: restraining moment induced by temperature crossfall

$$M_{ex+\Delta T}=M_{ex}+M_{\Delta T}$$

For the specimens of comparable series R, equivalent restraining moment was defined on the observed moment-curvature relationship assuming $\alpha=10\times10^{-6}/°C$.

(3) Measurement of Curvatures, Strains and Temperatures

Curvature of the specimen was determined by the deflections, which were measured by dial gauges with a minimum graduation of 1/100 mm. The measured curvatures were checked by the strains measured at the height 2 cm apart from the compression fiber and at the position of reinforcements.

A contact type strain gauge with a minimum graduation of 1/1 000 mm was used to measure the crack widths at the position of reinforcements. The gauge length between the contact points was 10 cm (see Fig. 2).

Strains in reinforcements were measured by foil type strain gauges with a gauge length of 2 mm, which were specially developed for the measurements of strains in the cryogenic conditions. To obtain the strain distributions of longitudinal reinforcements of L-3 specimen, ditches with a width of 4 mm and a depth of 2 mm were machined diametrically opposite on the bar to paste the strain gauges with a center distance of 2 cm, as is shown in Fig. 5.

Copper-constantan thermo-couples, which were located at the five sections shown in Fig. 1 and Fig. 6, were used to determine the temperture gradient across the height of the beam.

Average thermal expansion of concrete was calculated by the free curvature of beams and was approximated as the value of $10\times10^{-6}/°C$

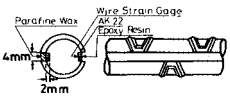

Fig. 5 Details of Instrumented Reinforcing Bar.

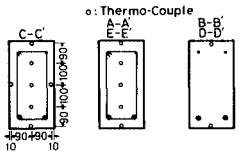

Fig. 6 Location of Thermo-Couples.

3. NUMERICAL COMPUTATION OF TEMPERATURE STRESSES AND CRACKS

(1) Material Properties

a) Concrete : Referring to the experimental results of water-saturated concrete obtained by Okada et al[11], Goto[12], Okazawa[13], Monfore et al[14], tensile strength ($\sigma_{tu}(T)$) and secant Young's modulus ($E_c(T)$), to be used for the numerical computation at the temperature (T), were assumed to be given as follows (see Fig. 7 and Fig. 8).

• Tensile strength

$$\sigma_{tu}(T)=|\sigma_{tu}|_{NT}+\Delta\sigma_{tu} \quad (kg/cm^2) \qquad \cdots\cdots (1)$$

$$T=(-8.167\times10^{-4}\,\Delta\sigma_{tu}^2+0.0155\,\Delta\sigma_{tu}-0.363)\Delta\sigma_{tu} \qquad (T\geqq T\geqq-100^\circ C)$$

$$\Delta\sigma_{tu}=0 \qquad (T\geqq0^\circ C)$$

• Young's modulus

$$E_c(T)=|E_c|_{NT}+\Delta E_c \quad (kg/cm^2) \qquad \cdots\cdots (2)$$

$$\Delta E_c=(8.095\,T-1090.5)T \qquad (0^\circ C\geqq T\geqq-100^\circ C)$$

$$\Delta E_c=0 \qquad (T\geqq0^\circ C)$$

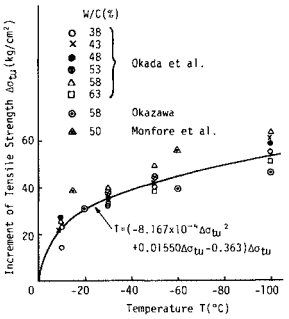

Fig. 7 Relationship between Increment of Tensile Strength of Concrete and Temperature.

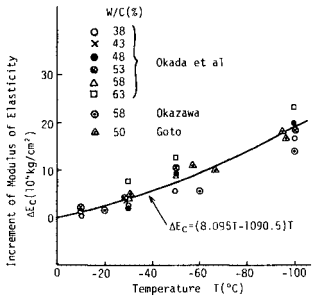

Fig. 8 Relationship between Increment of Modulus of Elasticity of Concrete and Temperature.

where, $|E_c|_{NT}$ and $|\sigma_{tu}|_{NT}$: Young's modulus and tensile strength of concrete at normal temperature, respectively.

b) Reinforcement : Young's modulus of reinforcements ($E_s(T)$) at the temperature T was also assumed to be the value at the normal temperature ($|E_s|_{NT}$) plus a additive value (ΔE_s) related to the effect of low temperatures[15].

$$E_s(T)=|E_s|_{NT}+\Delta E_s \quad (kg/cm^2) \qquad \cdots\cdots (3)$$

$$\Delta E_s=-594\,T \qquad (0^\circ C\geqq T\geqq-100^\circ C)$$

$$\Delta E_s=0 \qquad (T\geqq0^\circ C)$$

c) Bond stress-slip curve : Bond stress-slip curve ($\tau_x-\delta_x$) used for the numerical computation was determined based on the strain distribution measurements along the reinforcements in the specimen L-3. In Fig. 9 an example of the relationship between bond stresses (τ_x) and slip (δ_x) is shown for the case of temperature difference of $\Delta T=75.7^\circ C$ and $M_{ex+\Delta T}=10.88$ t-m(106.6 kN-m). Slips relative to surrounding concrete were assumed to be zero at the bottom of the valleys of strain distributions and the deformation of concrete was neglected.

Based on the test results the relationship between the temperatures at the position of reinforcements (T_r) and the bond strengths were approximated by the empirical curve shown in Fig. 10, and was used for the numerical computation of the general region excluding the portion adjacent to cracks.

Specifically for the portions near cracks in R as well as L specimens subjected to $M_{ex+\Delta T}$, as is shown in Fig. 11, bond strengths were assumed to decrease linearly to zero from the section 3.5 Ds apart from cracks (Ds stands for diameter of reinforcement.)[16]. Consequently, the bond strength in reinforcements is expressed as

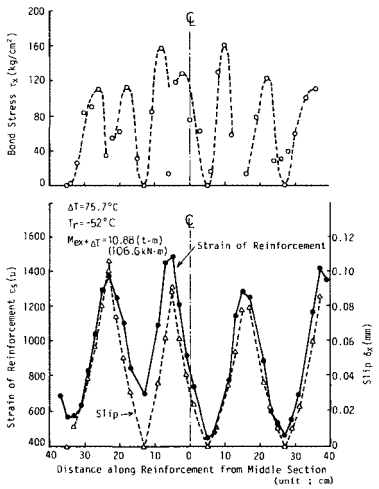

Fig. 9 Distributions of Bond Stress, Slip and Strain of Reinforcement.

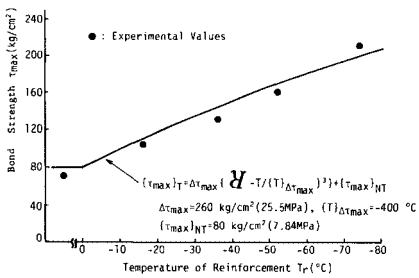

Fig. 10 Relationship between Maximum Bond Stress and Temperature of Reinforcement.

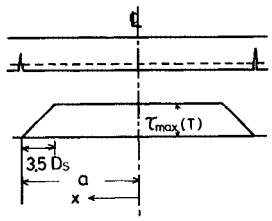

Fig. 11 Bond strength Distribution.

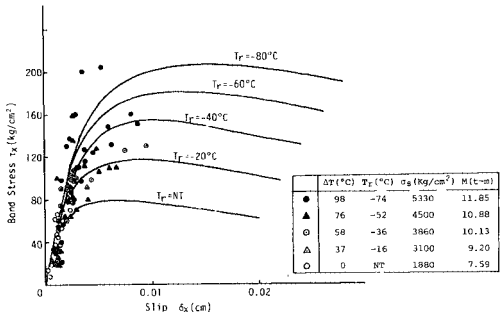

Fig. 12 Bond Stress-Slip Relationships under Thermal Gradient.

follows.

$$\left.\begin{aligned}&\tau_{max}(T_r,x)=\tau_{max}(T_r)[3.5\,D_s-|x-(a-3.5\,D_s)|]/3.5\,D_s \quad (a\geqq x\geqq a-3.5\,D_s)\\&\tau_{max}(T_r,x)=\tau_{max}(T_r) \quad (a-3.5\,D_s\geqq x\geqq 0)\end{aligned}\right\} \cdots\cdots (4)$$

Based on the experimental tendencies that bond rigidities that is, slopes of bond stresses to slips in the low bond stress region are almost independent of the temperature considered (see Fig. 12,), the slip ($\delta_{max}(T)$) at the peak of bond stress was supposed to be composed of the slip at normal temperature ($|\delta_{max}|_{NT}$) and the increment induced by the effect of temperature drop for the whole region along the beam ;

$$\left.\begin{aligned}&\delta_{max}(T_r)=\alpha_{max}\cdot T_r+|\delta_{max}|_{NT} \quad (0^\circ C\geqq T\geqq -80^\circ C)\\&\delta_{max}(T_r)=|\delta_{max}|_{NT} \quad (T\geqq 0^\circ C)\end{aligned}\right\} \cdots\cdots (5)$$

where, $\alpha_{max}=-0.001$ mm/°C, $|\delta_{max}|_{NT}=0.06$ mm

$\tau_x-\delta_x$ curves corresponding to several particular temperatures can be drawn such as those on Fig. 12, when the above mentioned experimental behaviors are incorporated in the type of formula proposed by Muguruma et al.[17]. The plotted points in the figure stand for the experimental values in the general area excluding the zones near cracks.

(2) Theoretical Procedures

a) Assumptions : Basic assumptions made for the theoretical computation are as follows ;

i) Concrete is an elastic as well as homogeneous material.

ii) "Plane sections remain plane" holds for the strains in concrete in compression zone and tensile reinforcements at an arbtitrary section of beam.

iii) Strains in concrete in tension zone is proportional to the distance from the neutral axis.

iv) All the cracks have the same width and are equally spaced, but these crack widths may be considered to be almost the same as the maximum ones.

v) Cracks are completely closed at the removal of loads and bond characteristics are not influenced by the loading histories.

vi) The temperature is linearly distributed along the height of the beam, keeping the temperature at compression fiber constant throughout the computation.

vii) Only flexural deformations due to temperature crossfall are restrained.

b) Basic equations : In the case of RC members subjected to temperature gradients, Young's modulus varies in the direction of the height of beam according to the distribution of temperatures at the moment considered. This is one of the main peculiar points when compared with the beams tested under a constant temperature.

Referring to Fig. 13 and applying the relationships in the equation (2), Young's modulus of concrete are derived as a function of distance z from the neutral axis ;

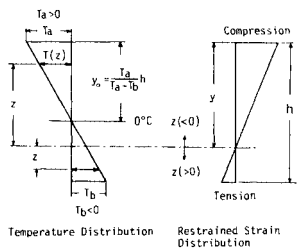

Fig. 13 An Example of Distributions of Temperature and Restrained Strain.

$$\left.\begin{aligned} E_c(z) &= g_1 z^2+(2g_1 y+g_2)z+g_1 y^2+g_2 y+g_3 \\ &\qquad (0^\circ C \geqq T \geqq -100^\circ C) \\ &= |E_c|_{NT} \qquad (T \geqq 0^\circ C) \end{aligned}\right\} \quad \cdots\cdots (6)$$

where,

$$g_1=\alpha_1 \{(T_b-T_a)/h\}^2$$
$$g_2=(2\alpha_1 T_a+\alpha_2)(T_b-T_a)/h$$
$$g_3=\alpha_1 T_a^2+\alpha_2 T_a+|E_c|_{NT}$$

From the experimental results, the coefficients, $\alpha_1=8.095$ and $\alpha_2=-1090.5$ were assumed. Given the strain distribution in the section, stresses in concrete can be obtained. A basic equation governing the mechanical behaviors in the active bond zone is expressed as follows, the derivation of which is given in reference 3).

$$\frac{d^2\delta_x}{dx^2}=\frac{U_s}{A_s E_s(T_r)}\cdot\{1-G(y)\}\tau_x \quad \cdots\cdots (7)$$

$$d\delta_x/dx=\varepsilon_s-\varepsilon_t=f(y) \quad \cdots\cdots (8)$$

Employing the type of function of $\tau_x-\delta_x$ proposed by Muguruma and Morita, equation (7) is reformed as follows.

$$\frac{d^2\delta_x}{dx^2}=\frac{U_s\cdot\tau_{max}(T_r,x)\cdot e}{A_s E_s(T_r)}\cdot\{1-G(y)\}\cdot\frac{\ln\{(e-1)\delta_x/\delta_{max}(T_r)+1\}}{(e-1)\delta_x/\delta_{max}(T_r)+1} \quad \cdots\cdots (9)$$

where, As and Us are cross sectional area and perimeter of tensile reinforcements, respectively. $G(y)$ is a function of the height of neutral axis y.

The above equation can be solved by using following boundary conditions on the premise that no bond splitting failures prevail along reinforcing bars. Based on the solution of the equation, restraining moments, flexural rigidities, stresses in reinforcements, crack widths, etc. are easily determined.

i) Perfect bond zone is present.

$x=0$; $\delta_x=0$, $d\delta_x/dx=0$

ii) Perfect bond zone is not present.

$x=0$; $\delta_x=0$ $\qquad$ $x=a$; $d\delta_x/dx=|\varepsilon_s|_{x=a}$ (cracked section)

4. EXPERIMENTAL BEHAVIORS OF THE BEAMS

(1) Cracking Behaviors

a) Distribution patterns of cracks : A typical post-failure cracking pattern of a RC beam, which was loaded under temperature gradient in low temperature region, is illustrated in Fig. 14 together with a companion beam tested under room temperature. The cracking behaviors of the beam subjected

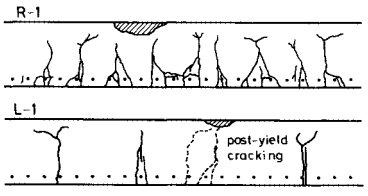

Fig. 14 Comparison of Crack Patterns Observed under Both External and Restraining Moments ($M_{ex+\Delta T}$) with Those Observed under External Moment (M_{ex}).

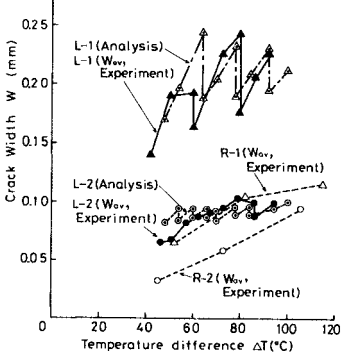

Fig. 15 Comparison of W_{av}-ΔT Relationships Measured under Restraining Moment ($M_{\Delta T}$) with Those Measured under External Moment (M_{ex}).

Table 2 Experimentally and Theoretically Obtained Number of Cracks.

	loading stages	moment M(t-m)	temp.diff. ΔT(°C)	number of cracks Exp.	Comput.
R-1	Mex	4.77	--------	15	7
	$M_{ex+\Delta T}$	5.73	91.9	3	4
L-1	Mex	2.05	0	3	3
	$M_{ex+\Delta T}$	4.74	48.9	3	6
R-2	Mex	9.55	--------	17	12
	$M_{ex+\Delta T}$	7.09	94.5	3	8
L-2	Mex	4.01	0	7	9
	$M_{ex+\Delta T}$	8.13	87.9	10	9
R-3	Mex	10.94	--------	13	12
L-3	Mex	7.59	0	11	9
	$M_{ex+\Delta T}$	11.85	98.2	11	9
R-4	Mex	14.64	--------	18	14
L-4	Mex	9.25	0	12	12
	$M_{ex+\Delta T}$	14.62	100.3	12	12

to temperature gradients are characterized by the wider crack spacings and fewer secondary cracks.

Table 2 shows the numbers of cracks observed in the specimens in the R and L series for the three loading stages. It is clear that when a beam is subjected to resraining moment in the absence of preceeding cracks, especially small number of cracks appear. Within the limit of the experiments, deformation was concentrated on the cracked sections even if the reinforcement ratio was doubled.

More finely distributed cracks were observed in the case of external moments combined with restraining moments and the phenomena may be attributable due to the effect of preceeding external moment at room temperature. However, the number of cracks are somewhat smaller than those of the specimens belonging to R series.

b) Width of cracks : Fig. 15 shows the change of average crack widths of RC beams (series L) subjected to only temperature gradients in comparison with those of the beams (series R) loaded under room temperature. Experimentally, in the case of the test under restraining moment only, the maximum crack widths had little difference compared with the average ones. Although in the case of L series newly developed cracks reduce widths of the existing ones, the values increased to the maximum of three times and two times as large as those of the beams belonging to R series with the reinforcement ratios of 0.57 % and 1.13 %, respectively. This indicates the fact that the seemingly favorable effects of improved material properties due to the exposure to freezing temperatures do not necessarily become conspicuous in terms of cracking behaviors.

The relationships between temperature differences and crack widths are depicted in Fig. 16 for the beam, which had been subjected to preceeding moment under room temperature (L-2) and that loaded at room temperature (R-2). Also experimental as well as theoretical crack widths are listed in Table 3 at the stages of several temperature differences.

The above experimental results indicate that, compared with the beams belonging to R series, the crack widths of the beams belonging to L series are likely to be smaller and larger in the cases of presence and absence of axial compressive forces, respectively. However, the difference is far less pronounced compared with the case in which the beams are subjected to only restraining moments.

Although the above experimental evidences infer that from the viewpoint of relationships between temperature differences and crack widths the effect of low temperature may be judged as unfavorable except for the case of the beams subjected to axial compression, the crack widths at the same reinforcement stress levels are even smaller than those of the beams tested at room temperature, notwithstanding the fact that the former has wider spacings of cracks (see Fig. 17).

The reason why the crack widths become larger in the case of the beams subjected to temperature gradient when compared at the same curvature under room temperature may be attributed to the fact that because of the remarkable increase in the flexural rigidities due to freezing effects the stresses in reinforcements also become increased, consequently, making the width of cracks wider. The experimental behaviors seem to indicate that conventional design method for control of crack widths,

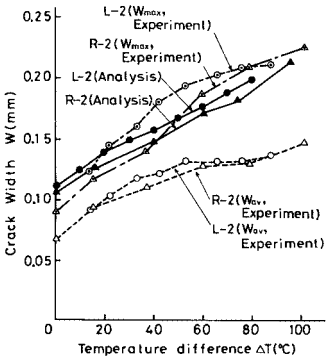

Fig. 16 Relationships between Temperature Differences (ΔT) and Crack Widths (W).

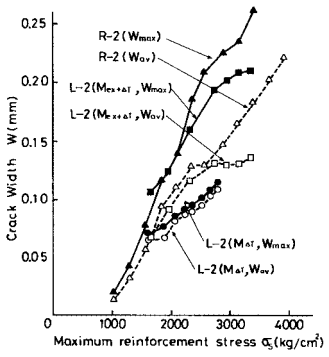

Fig. 17 Relationships between Maximum Stresses in Reinforcement (σ_s) and Crack Widths (W) (Experiment).

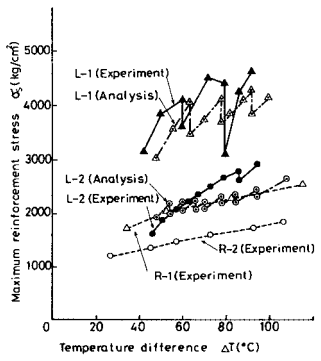

Fig. 18 Relationships between Temperature Differences (ΔT) and Maximum Stresses in Reinforcement (σ_s).

Table 3 Comparisons of Crack Widths Obtained from Experiments with Those from Numerical Computations.

Loading Stages	Specimens	ΔT=20°C Experiment Wav	ΔT=20°C Experiment Wmax	ΔT=20°C Comput.	ΔT=50°C Experiment Wav	ΔT=50°C Experiment Wmax	ΔT=50°C Comput.	ΔT=80°C Experiment Wav	ΔT=80°C Experiment Wmax	ΔT=80°C Comput.
$M_{\Delta T}$	L-1				0.19	0.19	0.18	0.18	0.21	0.20
	R-1				0.06	0.10	0.12	0.10	0.13	0.15
	L-2				0.07	0.08	0.09	0.10	0.11	0.09
	R-2				0.04	0.05	0.06	0.07	0.09	0.09
$M_{ex+\Delta T}$	L-1	0.15	0.18	0.18	0.26	0.29	0.24			
	R-1	0.11	0.14	0.17	0.15	0.20	0.25	0.15	0.26	0.31
	L-2	0.10	0.14	0.14	0.13	0.19	0.17	0.13	0.21	0.20
	R-2	0.10	0.12	0.13	0.12	0.17	0.16	0.13	0.21	0.19
	L-3	0.11	0.13	0.19	0.16	0.18	0.25	0.19	0.23	0.30
	R-3	0.12	0.17	0.14	0.17	0.26	0.20	0.21	0.34	0.25
	L-4	0.09	0.13	0.13	0.12	0.17	0.16	0.14	0.19	0.19
	R-4	0.09	0.14	0.12	0.12	0.18	0.15	0.14	0.22	0.18

Wav, Wmax: Average and maximum crack widths, respectively. (unit: mm)

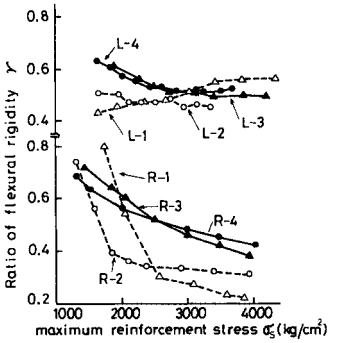

Fig. 19 Relationships between Maximum Stresses in Reinforcement (σ_s) and Ratios of Flexural Rigidiies (γ).

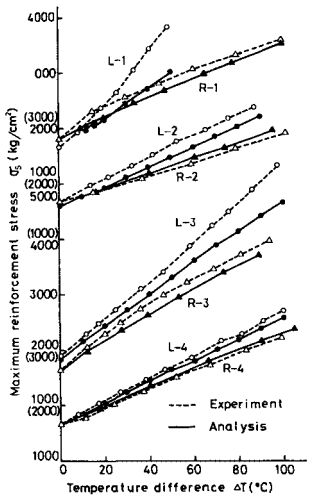

Fig. 20 Relationships between Temperature Differences (ΔT) and Maximum Stresses in Reinforcement (σ_s).

which is mainly based on the stresses in reinforcements, give rather conservative results, compared with those for the cases under normal temperatures.

The ratios between measured and calculated average crack widths (W_{av}) are 1.31 and 1.46 for L and R series specimens, respectively, while corresponding ratios for maximum crack widths (W_{max}) are 1.04 and 1.03, respectively.

(2) Temperature Stresses

In Fig. 18, comparisons are made of the relationships between temperature gradients (or equivalent gradient) and stresses in reinforcements for the RC beams subjected to only temperature gradient (L series) and those tested under normal temperature (R series). As was explained in the previous section, the stresses in reinforcements in L series considerably exceed those in R series, constituting one of the important reasons to increase the crack widths in the specimens belonging to L series.

Considering the fact that the most of the compression zone of the beams was kept above freezing point, the remarl able increase in flexural rigidities observed in the tests may be attributable to the improvements in the tensile strength of concrete as well as bond strength between steel and concrete, which was caused by the effect of freezing temperatures.

Steel stress dependent on rngidity reduction indexes γ (defined as a ratio of measured flexural regidity after cracking to that based on gross section assuming the material properties at room temperature) are depicted in Fig. 19 for the beams subjected to restraining moment combined with the preceeding external moment in comparison with those tested at room temperature. As is seen from the figure, although the values of γ for R series monotonically decrease with increment in steel stresses, γ for the beams placed under temperature gradient superimposed by external moments are almost unchanged up to yielding points of steel in spite of the presence of rather finely distributed cracks caused by the previously applied external moment at room temperature.

The rigidity reduction indexes γ at room temperature are generally higher when axial compressive forces as well as larger amount of tensile steels are present. The values of γ corresponding to the beams under temperature gradient in the freezing temperature regions, however, are almost constant between 0.4 and 0.6, being not influenced by the presence of axial forces as well as the amount of tensile reinforcements.

Experimentally obtained maximum reinforcement stresses are compared with computed values in

Fig. 20. This figure clearly shows the experimental behaviors, that the difference of γ between the two cases of L and R series is more pronounced as the reinforcement ratio become lower. Also, the agreement of computed results with experimental ones may be found fairly good, taking the complexities involved in the problem into account.

5. CONCLUSIONS

To help rationalize the design of the reinforced concrete structures such as underground tanks for storage of LNG, in which temperature effect plays an important role, an experimental study was conducted in which RC beams were subjected to flexural moment under temperature gradients in the low temperature regions. Also, an theoretical approach was applied to estimate the mechanical behaviors of beams such as temperature stresses, widths of cracks, etc. taking into consideration the change of material properties caused by freezing effects. The followings are the main conclusions obtained within the limit of the study.

(1) The number of cracks caused by the effect of temperature gradient induced moment in the low temperature regions was only three in the test region of 210 cm for the beams with reinforcement rations of 0.57 % as well as 1.13 %. The average spacings of cracks were 5 to 6 times as large as those obtained in the tests conducted in the normal temperature region. This may point the importance of artificially distributing cracks to avoid concentration of cracks in the freezing temperature regions.

(2) The maximum stresses in tensile reinforcements caused only by temperature gradient were approximately 2.0 and 1.6 times as large as those occuring in the companion beams with reinforcement ratios of 0.57 % and 1.13 %, respectively, which were tested under room temperature, when comparisons were made at the same restraining curvatures. The corresponding ratios for crack widths were about 2.4 and 2.0, respectively. The experimental evidence clearly showed the differences of influences of temperature gradients under normal and freezing temperature regions.

(3) The flexural regidity reduction indexes γ of the beams, which had been subjected to flexural moment at room temperature and were subsequently to temperature gradients, were found to be constant between 0.4~0.6, from the stress levels of concrete cracking to yielding in steel, being independent of the presence or absence of axial forces as well as the values of reinforcement rations. The discrepancies between γ of the beams loaded under room temperature and those of the beams exposed to freezing effects are more pronounced, the lower the reinforcement ratios and the amount of axial compression forces.

(4) From the viewpoint of the relationships between stresses in reinforcements and crack widths, however, the widths of cracks observed in the frozen state were somewhat smaller than those obtained under room temperature at the same level of stresses in reinforcements. As a result, it may be suggested that conventional design procedures for controlling crack widths, which are constructed as a function of steel stresses, can be applied also somewhat conservatively to the cases where RC flexural members are subjected to temperature gradiets in freezing temperatures.

(5) The proposed theoretical approach, in which the temperature-dependent changes of mechanical properties of concrete and steel as well as bond-slip characteristics between reinforcement and concrete can be taken into account, was found to be effective in estimating the stresses in reinforcements, crack widths, etc. of RC beams subjected to temperature crossfall in freezing conditions, including the cases of simultaneous actions of axial forces and external moments.

The validity of the method was substantiated in the light of comparisons between experimental and theoretical results. The extention of the proposed method deems promissing even to the cases where RC members are subjected to elevated temperature effect by providing appropriate material properties.

6. ACKNOWLEDGEMENT

The first author wishes to acknowledge the eager encouragement that he received from professor Dr. S. Nagataki of Tokyo Institute of Technology.

The authors also express their gratitudes to H. Kusaka, M. Kurebayashi and S. Itoh for their cooperation in the experimental works.

REFERENCE

1) Okada, T., Imai, M., Nagasawa, Y., Ishikawa, N. and Kimura, K. : Flexural Behaviors of Concrete Beams at Low Temperature, Concrete Journal, Vol. 15, No. 11, pp. 9~20, Nov. 1977 (in Japanese).
2) Goto, Y. and Miura, T. : Mechanical Properties of Reinforced Concrete Members at Very Low Temperatures, Proceedings of JSCE, No. 285, pp. 121~134, May 1979 (in Japanese).
3) Sato, R. and Aoyagi, Y. : Studies on Deformation and Crack of Reinforced Concrete Flexural Members under Low Temperature, Proceedings of JSCE, No. 329, pp. 141~154, Jan. 1983.
4) ACI Committee 307 : Specification for the Design and Construction of Reinforced Concrete Chimneys, ACI Journal, Proceedings Vol. 65, No. 9, pp. 689~712, Sept. 1968.
5) Gurfinkel, G. : Thermal Effects in Walls of Nuclear Containments-Elastic and Inelastic Behavior, Proceedings of the 1-st International Conference on Structural Mechanics in Reactor Technology, Paper J 3/7, pp. 277~297, Aug. 1971.
6) Pajuhesh, J. : Thermal Relaxation in Concrete Structure, ACI Journal, Proceedings Vol. 73, No. 9, pp. 522 ~ 525, Sept. 1976.
7) Larrabee, R. D., Billington, D. P. and Abel, J. F. : Thermal Loading of Thin-Shell Concrete Cooling Towers, Journal of the Structural Division, Proceedings of ASCE, Vol. 100, No. ST 12, pp. 2367~2383, Dec. 1974.
8) AGI Committee 313 : Recommended Practice for Design and Construction of Concrete Bins, Silos and Bunkers for Storing Granular Materials, ACI Journal, Proceedings Vol. 72, No. 10, pp. 529~548, Sept. 1975.
9) Aoyagi, Y., Onuma, H. and Okazawa, T. : Experimental Study on the Cracking Behaviors of Reinforced Concrete Hollow Cylinders Subjected to Temperature Gradient and the Assessment of Decrease in Flexural Rigidity due to Cracking, Technical Report of Central Research Institute of Electric Power Industry, No. 376002, 56 p, Oct. 1976 (in Japanese).
10) Inomata, S. : An Estimation of Temperature Gradient Induced Moments for Reinforced Concrete Members, Personal correspondence, not published.
11) Noakowski, P. : Bemessung auf Biegezwang in Hinblick auf zulassige Stahlspannung und zulassige Riβbreit, Bauingnieur, 52. Jahr., Heft 4, pp. 137~144. Apr. 1977.
12) Goto, Y. : Physical Properties of Concrete at Very Low Temperatures, Concrete Journal, Vol. 15, No. 11, pp. 1 ~ 8, Nov. 1977 (in Japanese).
13) Okazawa, T. : Strength of Concrete under Very Low Temperature and under Low Temperature Cycle, Technical Report of Central Research Institute of Electric Power Industry, No. 379017, 17 p, Feb. 1980 (in Japanese).
14) Monfore, G. E. and Lenz, A. E. : Physical Properties of Concrete at Very Low Temperatures. Journal of PCA Research and Development Lab. Vo. 4, No. 2, pp. 33~39, May 1962.
15) Numazaki, Y. : Experimental Studies on Strengths of Deformed Bars and Those Joints under Low Temperatures, Request Report of Central Research Institute Electric Power Industry, No. 378519, 43 p, Aug. 1978 (in Japanese).
16) Kokusho, S., Hayashi, S., Kobayashi, K. and Yoshida, H. : Basic Study on Bond between Deformed Bar and Concrete, Summaries of Technical Papers of Annual Meeting of AIJ, pp. 1327~1328, Oct. 1982 (in Japanese)
17) Muguruma, H., Morita, S. and Tomita, K. : Fundamental Study on Bond between Steel and Concrete (Part 1), Transactions of AIJ, No. 131, pp. 1~8, Jan. 1967, No. 132, pp, 1~6, Feb. 1967 (in Japanese).

(Recieved. January 25. 1984)